Research Article | Vol. 7, No. 12 | 1 Dec 2016 | BIOMEDICAL OPTICS EXPRESS 4982

Biomedical Optics EXPRESS

Supra-organization and optical anisotropies of the extracellular matrix in the amniotic membrane and limbal stroma before and after explant culture

GISELE P. VALDETARO,[1] MARCELA ALDROVANI,[1,*] IVAN R. M. PADUA,[1] PRISCILA C. CRISTOVAM,[2] JOSÉ A. P. GOMES,[2] AND JOSÉ L. LAUS[1]

[1]*Ophthalmology Unit, Department of Small Animal Medicine and Surgery, Faculty of Agrarian and Veterinary Sciences, UNESP Jaboticabal, 14884-900, SP, Brazil*
[2]*Ocular Surface Advanced Center, Federal University of São Paulo, UNIFESP São Paulo, 04039-002, SP, Brazil*
[*]*marcela.aldrovani@gmail.com*

Abstract: In this research we evaluated the supramolecular organizations and the optical anisotropical properties of the de-epithelialized human amniotic membrane and rabbit limbal stroma, before and after explant culture. Birefringence, monochromatic light spectral absorption and linear dichroism of the main extracellular matrix biopolymers, that is, the fibrillar collagens and proteoglycans, were investigated by polarized light microscopy combined with image analysis. Our results demonstrated that the culture procedure–induced stimuli altered the supra-organizational characteristics (in terms of collagens/proteoglycans spatial orientation and ordered-aggregational state) of the amniotic and limbal extracellular matrix, which led to changes in optical anisotropical properties.

OCIS codes: (000.1430) Biology and medicine; (170.4470) Ophthalmology; (160.1190) Anisotropic optical materials; (260.5430) Polarization; (260.1440) Birefringence; (100.1930) Dichroism.

References and links

1. O. Baylis, F. Figueiredo, C. Henein, M. Lako, and S. Ahmad, "13 years of cultured limbal epithelial cell therapy: a review of the outcomes," J. Cell. Biochem. **112**(4), 993–1002 (2011).
2. M. E. Rendal-Vázquez, A. San-Luis-Verdes, M. T. Yebra-Pimentel-Vilar, I. López-Rodríguez, N. Domenech-García, C. Andión-Núñez, and F. Blanco-García, "Culture of limbal stem cells on human amniotic membrane," Cell Tissue Bank. **13**(3), 513–519 (2012).
3. W. Li, Y. Hayashida, Y. T. Chen, and S. C. Tseng, "Niche regulation of corneal epithelial stem cells at the limbus," Cell Res. **17**(1), 26–36 (2007).
4. J. Ovadia and Q. Nie, "Stem cell niche structure as an inherent cause of undulating epithelial morphologies," Biophys. J. **104**(1), 237–246 (2013).
5. G. Pellegrini and M. De Luca, "Eyes on the prize: limbal stem cells and corneal restoration," Cell Stem Cell **15**(2), 121–122 (2014).
6. L. J. Cooper, S. Kinoshita, M. German, N. Koizumi, T. Nakamura, and N. J. Fullwood, "An investigation into the composition of amniotic membrane used for ocular surface reconstruction," Cornea **24**(6), 722–729 (2005).
7. H. Mei, S. Gonzalez, and S. X. Deng, "Extracellular matrix is an important component of limbal stem cell niche," J. Funct. Biomater. **3**(4), 879–894 (2012).
8. S. Chen, M. J. Mienaltowski, and D. E. Birk, "Regulation of corneal stroma extracellular matrix assembly," Exp. Eye Res. **133**(1), 69–80 (2015).
9. N. K. Weidenhamer, D. L. Moore, F. L. Lobo, N. T. Klair, and R. T. Tranquillo, "Influence of culture conditions and extracellular matrix alignment on human mesenchymal stem cells invasion into decellularized engineered tissues," J. Tissue Eng. Regen. Med. **9**(5), 605–618 (2015).
10. E. Mattia and S. Otto, "Supramolecular systems chemistry," Nat. Nanotechnol. **10**(2), 111–119 (2015).
11. P. Rifes and S. Thorsteinsdóttir, "Extracellular matrix assembly and 3D organization during paraxial mesoderm development in the chick embryo," Dev. Biol. **368**(2), 370–381 (2012).
12. K. Burridge and M. Chrzanowska-Wodnicka, "Focal adhesions, contractility, and signaling," Annu. Rev. Cell Dev. Biol. **12**(1), 463–519 (1996).
13. J. Hao, Y. Zhang, D. Jing, Y. Shen, G. Tang, S. Huang, and Z. Zhao, "Mechanobiology of mesenchymal stem cells: Perspective into mechanical induction of MSC fate," Acta Biomater. **20**(20), 1–9 (2015).
14. H. Lv, L. Li, Y. Zhang, Z. Chen, M. Sun, T. Xu, L. Tian, M. Lu, M. Ren, Y. Liu, and Y. Li, "Union is strength: matrix elasticity and microenvironmental factors codetermine stem cell differentiation fate," Cell Tissue Res. **361**(3), 657–668 (2015).

#265072 http://dx.doi.org/10.1364/BOE.7.004982
Journal © 2016 Received 13 Jun 2016; revised 8 Aug 2016; accepted 10 Aug 2016; published 7 Nov 2016

Biomedical Optics EXPRESS

15. C. S. Chen, J. Tan, and J. Tien, "Mechanotransduction at cell-matrix and cell-cell contacts," Annu. Rev. Biomed. Eng. **6**(1), 275–302 (2004).
16. J. Schiller and D. Huster, "New methods to study the composition and structure of the extracellular matrix in natural and bioengineered tissues," Biomatter **2**(3), 115–131 (2012).
17. L. C. Palmer, Y. S. Velichko, M. O. de la Cruz, and S. I. Stupp, "Supramolecular self-assembly codes for functional structures," Philos. Trans. A Math Phys. Eng. Sci. **365**(1855), 1417–1433 (2007).
18. J. M. Lehn, "Toward self-organization and complex matter," Science **295**(5564), 2400–2403 (2002).
19. M. J. Webber, J. A. Kessler, and S. I. Stupp, "Emerging peptide nanomedicine to regenerate tissues and organs," J. Intern. Med. **267**(1), 71–88 (2010).
20. S. L. Jacques, "Optical properties of biological tissues: a review," Phys. Med. Biol. **58**(11), R37–R61 (2013).
21. S. N. Savenkov, O. I. Sydoruk, and R. S. Muttiah, "Conditions for polarization elements to be dichroic and birefringent," J. Opt. Soc. Am. A **22**(7), 1447–1452 (2005).
22. D. F. da Silva, B. C. Vidal, D. M. Zezell, T. M. Zorn, S. C. Núñez, and M. S. Ribeiro, "Collagen birefringence in skin repair in response to red polarized-laser therapy," J. Biomed. Opt. **11**(2), 024002 (2006).
23. M. Aldrovani, A. M. A. Guaraldo, and B. C. Vidal, "Optical anisotropies in corneal stroma collagen fibers from diabetic spontaneous mice," Vision Res. **47**(26), 3229–3237 (2007).
24. B. C. Vidal and M. L. S. Mello, "Optical anisotropy of collagen fibers of rat calcaneal tendons: An approach to spatially resolved supramolecular organization," Acta Histochem. **112**(1), 53–61 (2010).
25. J. F. Ribeiro, E. H. dos Anjos, M. L. S. Mello, and B. de Campos Vidal, "Skin collagen fiber molecular order: a pattern of distributional fiber orientation as assessed by optical anisotropy and image analysis," PLoS One **8**(1), e54724 (2013).
26. B. C. Vidal, "Form birefringence as applied to biopolymer and inorganic material supraorganization," Biotech. Histochem. **85**(6), 365–378 (2010).
27. H. S. Bennett, "The microscopical investigation of biological materials with polarized light," in *McClung's Handbook of Microscopical Technique, E. D.* Jones, ed. (Hafner Publ. Co, 1967).
28. J. Y. Cassim, P. S. Tobias, and E. W. Taylor, "Birefringence of muscle proteins and the problem of structural birefringence," Biochim. Biophys. Acta **168**(3), 463–471 (1968).
29. S. Roth and I. Freund, "Optical second-harmonic scattering in rat-tail tendon," Biopolymers **20**(6), 1271–1290 (1981).
30. S. Roth and I. Freund, "Second harmonic-generation and orientational order in connective tissue: a mosaic model for fibril orientational ordering in rat tailtendon," J. Appl. Cryst. **15**(1), 72–78 (1982).
31. B. C. Vidal, "Pleochroism in tendon and its bearing to acid mucopolysaccharides," Protoplasma **56**(4), 529–536 (1963).
32. B. C. Vidal, "The part played by the mucopolysaccharides in the form birefringence of collagen," Protoplasma **59**(3-4), 472–479 (1965).
33. M. L. S. Mello and B. C. Vidal, "Anisotropic properties of toluidine blue-stained collagen," Ann. Histochim. **18**(2), 103–122 (1973).
34. V. Louis-Dorr, K. Naoun, P. Allé, A. M. Benoit, and A. Raspiller, "Linear dichroism of the cornea," Appl. Opt. **43**(7), 1515–1521 (2004).
35. A. Aparecida de Aro, B. C. Vidal, and E. R. Pimentel, "Biochemical and anisotropical properties of tendons," Micron **43**(2-3), 205–214 (2012).
36. R. R. Loureiro, P. C. Cristovam, C. M. Martins, J. L. Covre, J. A. Sobrinho, J. R. Ricardo, R. M. Hazarbassanov, A. L. Höfling-Lima, R. Belfort, Jr., M. Nishi, and J. Á. Gomes, "Comparison of culture media for ex vivo cultivation of limbal epithelial progenitor cells," Mol. Vis. **19**(1), 69–77 (2013).
37. B. C. Vidal and M. L. S. Mello, "Supramolecular order following binding of the dichroic birefringent sulfonic dye Ponceau SS to collagen fibers," Biopolymers **78**(3), 121–128 (2005).
38. R. Lattouf, R. Younes, D. Lutomski, N. Naaman, G. Godeau, K. Senni, and S. Changotade, "Picrosirius red staining: a useful tool to appraise collagen networks in normal and pathological tissues," J. Histochem. Cytochem. **62**(10), 751–758 (2014).
39. S. L. Dallas, Q. Chen, and P. Sivakumar, "Dynamics of assembly and reorganization of extracellular matrix proteins," Curr. Top. Dev. Biol. **75**(1), 1–24 (2006).
40. J. M. Bueno and F. Vargas-Martín, "Measurements of the corneal birefringence with a liquid-crystal imaging polariscope," Appl. Opt. **41**(1), 116–124 (2002).
41. M. M. Giraud-Guille, L. Besseau, and R. Martin, "Liquid crystalline assemblies of collagen in bone and in vitro systems," J. Biomech. **36**(10), 1571–1579 (2003).
42. M. M. Giraud Guille, G. Mosser, C. Helary, and D. Eglin, "Bone matrix like assemblies of collagen: from liquid crystals to gels and biomimetic materials," Micron **36**(7-8), 602–608 (2005).
43. B. C. Vidal and M. L. S. Mello, "Structural organization of collagen fibers in chordae tendineae as assessed by optical anisotropic properties and Fast Fourier transform," J. Struct. Biol. **167**(2), 166–175 (2009).
44. N. J. Jan, J. L. Grimm, H. Tran, K. L. Lathrop, G. Wollstein, R. A. Bilonick, H. Ishikawa, L. Kagemann, J. S. Schuman, and I. A. Sigal, "Polarization microscopy for characterizing fiber orientation of ocular tissues," Biomed. Opt. Express **6**(12), 4705–4718 (2015).
45. B. C. Vidal and P. L. O. Volpe, "Differential scanning calorimetry and optical properties of collagen-dichroic azo ponceau SS complexes," Braz. J. Morphol. Sci. **22**(3), 149–150 (2005).
46. D. F. Silva, A. S. Gomes, B. de Campos Vidal, and M. S. Ribeiro, "Birefringence and second harmonic generation on tendon collagen following red linearly polarized laser irradiation," Ann. Biomed. Eng. **41**(4), 752–762 (2013).

Biomedical Optics EXPRESS

47. R. Vilarta and B. C. Vidal, "Anisotropic and biomechanical properties of tendons modified by exercise and denervation: aggregation and macromolecular order in collagen bundles," Matrix **9**(1), 55–61 (1989).
48. F. Gattazzo, A. Urciuolo, and P. Bonaldo, "Extracellular matrix: a dynamic microenvironment for stem cell niche," Biochim. Biophys. Acta **1840**(8), 2506–2519 (2014).
49. J. R. García and A. J. García, "Cellular mechanotransduction: sensing rigidity," Nat. Mater. **13**(6), 539–540 (2014).
50. L. Li, N. Sharma, U. Chippada, X. Jiang, R. Schloss, M. L. Yarmush, and N. A. Langrana, "Functional modulation of ES-derived hepatocyte lineage cells via substrate compliance alteration," Ann. Biomed. Eng. **36**(5), 865–876 (2008).
51. Q. Tseng, E. Duchemin-Pelletier, A. Deshiere, M. Balland, H. Guillou, O. Filhol, and M. Théry, "Spatial organization of the extracellular matrix regulates cell-cell junction positioning," Proc. Natl. Acad. Sci. U.S.A. **109**(5), 1506–1511 (2012).
52. K. M. Meek and N. J. Fullwood, "Corneal and scleral collagens--a microscopist's perspective," Micron **32**(3), 261–272 (2001).
53. C. Boote, S. Dennis, and K. Meek, "Spatial mapping of collagen fibril organisation in primate cornea-an X-ray diffraction investigation," J. Struct. Biol. **146**(3), 359–367 (2004).
54. J. W. Jaronski and H. T. Kasprzak, "Linear birefringence measurements of the in vitro human cornea," Ophthalmic Physiol. Opt. **23**(4), 361–369 (2003).
55. T. Kawakita, E. M. Espana, H. He, W. Li, C. Y. Liu, and S. C. Tseng, "Intrastromal Invasion by Limbal Epithelial Cells Is Mediated by Epithelial-Mesenchymal Transition Activated by Air Exposure," Am. J. Pathol. **167**(2), 381–393 (2005).
56. W. Li, Y. Hayashida, H. He, C. L. Kuo, and S. C. Tseng, "The fate of limbal epithelial progenitor cells during explant culture on intact amniotic membrane," Invest. Ophthalmol. Vis. Sci. **48**(2), 605–613 (2007).
57. P. Whittaker, D. R. Boughner, and R. A. Kloner, "Analysis of healing after myocardial infarction using polarized light microscopy," Am. J. Pathol. **134**(4), 879–893 (1989).
58. B. C. Vidal, "Image analysis of tendon helical superstructure using interference and polarized light microscopy," Micron **34**(8), 423–432 (2003).
59. Y. M. Michelacci, "Collagens and proteoglycans of the corneal extracellular matrix," Braz. J. Med. Biol. Res. **36**(8), 1037–1046 (2003).
60. A. Redaelli, S. Vesentini, M. Soncini, P. Vena, S. Mantero, and F. M. Montevecchi, "Possible role of decorin glycosaminoglycans in fibril to fibril force transfer in relative mature tendons--a computational study from molecular to microstructural level," J. Biomech. **36**(10), 1555–1569 (2003).
61. R. V. Iozzo, "Matrix proteoglycans: from molecular design to cellular function," Annu. Rev. Biochem. **67**(1), 609–652 (1998).
62. L. Gomes, M. A. Esquisatto, P. Belline, and E. R. Pimentel, "Is there a relationship between the state of aggregation of small proteoglycans and the biomechanical properties of tissues?" Braz. J. Med. Biol. Res. **29**(9), 1243–1246 (1996).
63. M. Silbermann and J. Frommer, "Dynamic changes in acid mucopolysaccharides during mineralization of the mandibular condylar cartilage," Histochemie **36**(2), 185–192 (1973).

1. Introduction

Amniotic membranes containing limbal epithelial progenitor cells (LEPCs) expanded by explant culture are among the bioengineered constructs most used in ocular surface reconstruction [1]. Membranes and LEPCs/explants can be derived from different species; called xenografts, they have already been proven viable [2]. Xenografts are routinely used in basic research since key information on LEPC properties and therapeutic potential has been provided by studies associating de-epithelialized human amniotic membrane (dHAM) and rabbit limbus [2].

Studies have attempted to evaluate the composition of extracellular matrix (ECM) of dHAM by comparison with the limbal stromal ECM. The primary goal is establishing the role of each extracellular component in the complex microenvironmental regulation program, by which LEPCs do or do not retain undifferentiated traits. Many oligomers of ECM biopolymers related to cell signaling pathways (e.g. Wnt/β-catenin, TGF-β/BMP, Sonic hedgehog, Notch, Ras/MAPK, PI3K/Akt, and other) have been detected by immunohistochemistry [3–5]. Conversely, the supramolecular organizations of ECM have been little investigated. Fibrillary collagens and proteoglycans (PGs) represent the main supra-organized biopolymers in amniotic and limbal stromal ECMs [6–8].

The term supramolecular organization (or supra-organization) refers to the arrangement of the biopolymer that confers a structure's macroscopic and biomechanical attributes [9, 10]. Based on previous reports [11], we have hipothesized that supramolecular organizations of the dHAM and limbal stromal ECM could be drastically altered by explant culture procedures. To evaluate this hypothesis is important because supra-organizations of ECM generates some

Biomedical Optics EXPRESS

temporal and spatial physical properties that modulate cell behavior, such as geometry, threedimensional orientation, surface topography, stiffness, and mechanical strength [12–15]. Furthermore, supramolecular organizations first started to be considered among the full hierarchic levels that researchers must master to create artificial tissues or membranes after the advent of nanobiotechnology [16–19]. In ophthalmology, evaluating a supra-organization and later reproducing it in a laboratory has become reality.

Supra-organized ECM biopolymers contains morpho-functional requirements at the nanoscale level [16, 17]. In addition, they display important optical anisotropic properties, which result from elements that are periodically ordered at the atomic and molecular levels [20]. The incidence of polarized electromagnetic waves on anisotropic structures leads to measurable changes in phase or amplitude of the orthogonal components of the electric vector, known as birefringence and dichroism, respectively [20–25]. Studies on birefringence and dichroim (using polarized light microscope and image analysis) inform us as supramolecular organizations react with adaptation and flexibility to the morpho-functional or pathological requirements [26]. For example, several authors detected changes in supra-organization and anisotropical properties of ECM during wound healing, aging, endochondral ossification, inflammation and osteoarthritis, gelatinous drop-like corneal dystrophy, keratoconus, diabetes, floppy mitral valve syndrome and other.

Birefringence is one of the optical effects of anisotropy. It results from the material's difference in refractive indexes that leads to light propagation in different speeds and directions [20, 23, 24, 26–30]. Regarding ECM, birefringence informs us on the supra-organization of the fibrillary collagens (in terms of fiber spatial orientation and ordered aggregational state) and is formed of two fractions: intrinsic and form birefringence. Intrinsic birefringence is expressed by the equation $n_e - n_o$, where n_e is the refractive index in the direction of propagation of the extraordinary ray and n_o is the refractive index in the direction of the ordinary ray. It results from the electronic transitions of peptide bonds along the fiber axis [22, 26–30]. Form birefringence results from the compatibility of the photon's wavelengths and the nanometric dimensions of asymmetrical molecules in the fibrillary collagens [24–32]. It can be considered a nonlinear optical property [26–30].

Dichroism is an anisotropy of spectral absorption that manifests in changes in the amplitude of the electric vector of the polarized light [23, 27, 33–35]. Dichroic macromolecules absorb polarized light differently according to the direction of their chromophoric groups in relation to the plane polarized light (PPL) [23, 31, 32]. In ECM studies, the phenomenon of linear dichroism (LD) can be extrinsically obtained using topo-optical staining with thiazine, which allows us to establish the spatial orientation of the glycosaminoglycans (GAGs) of PGs in relation to the long axis of the collagen fibers [32, 33].

The aim of this research was to evaluate the supramolecular organizations of the dHAM and limbal stromal ECM, before and after explant culture. For this, the anisotropic properties (birefringence and LD/spectral absorption) of the main ECM structural biopolymers, that is, the fibrillar collagens and PGs, were studied using polarized linearly light microscope.

2. Methods

2.1. Human amniotic membrane processing

Amniotic membrane was obtained after written informed consent from the prospective mother, upon her cesarean-section delivery and prepared under sterile conditions, washed with a balanced saline solution containing penicillin, streptomycin, neomycin and amphotericin B (Ophthalmos, Sao Paulo, Brazil), placed over a nitrocellulose membrane and preserved in Dulbecco's Modified Eagle medium (DMEM; Sigma-Aldrich, St. Louis, MO, USA) and glycerol (Ecibra, Sao Paulo, Brazil) at a ratio of 1:1 at −80°C. Prior to amniotic membrane use, it was thawed at room temperature, detached from the nitrocellulose membrane (Merck Millipore, Darmstadt, Germany), and washed three times in phosphate buffered saline. In order to remove epithelia, amniotic membrane was incubated with ethylenediaminetetraacetic acid (Sigma-Aldrich) 0.02% during 2 h, at 37°C, where upon the

Biomedical Optics EXPRESS

epithelia were mechanically removed. The amniotic membrane was cut into 24 fragments measuring 2x2 cm. Eighteen dHAM fragments were destined for the cell culture procedures, while the remaining fragments (uncultured controls) were used to create the histological sections.

2.2. Animals and limbus biopsy

The study adhered to the Statement for Use of Animals in Ophthalmic Vision and Research by the Association for Research in Vision and Ophthalmology (ARVO). The ethical principles established by the Canadian Council on Animal Care (Principles of Laboratory Care, NIH publication number 85-23 revised in 1996) were followed. Six adult male and female New Zealand White rabbits were used.

The limbus biopsy on the rabbits was performed under dissociative anesthesia (xylazine and ketamine). The cornea was desensitized with tetracaine ophthalmic drops containing 0.1% phenylephrine (Allergan, Sao Paulo, Brazil). Two corneoscleral limbus fragments were removed from the right eye of each rabbit under the guidance of a surgical microscope (DF Vasconcelos, Sao Paulo, Brazil). Limbus explants measuring 2x2 mm were collected from the 10 to 12 o'clock and 4 to 6 o'clock positions using a 15° angle blade (Alcon, Sao Paulo, Brazil) and stainless steel tweezers (Colibri, Sao Paulo, Brazil). Biopsy size was established using a caliper. The endothelium and posterior stroma (about 2/3) of the limbus were discarded and the explants were subsequently divided into two equal halves. Eighteen limbus fragments were destined for cell culture on dHAM. The remaining (uncultured controls) were used to make histological sections.

2.3. Explant culture

Limbus fragments were accommodated on the dHAM fragments with the epithelium facing upward. The culture conditions (5% CO_2 incubator at a constant temperature of 37°C) and media were identical for all samples: DMEM/HAM-F12 containing 10% fetal calf serum, 0.5% dimethyl sulfoxide, sodium selenite 5 ng/mL, apo-transferrin 5 µg/mL, epidermal growth factor 2 ng/mL, cholera toxin 0.1 µg/mL, insulin 1 µg/mL, hydrocortisone 5 µg/mL, penicillin, streptomycin, and amphotericin B [36]. All tissue culture reagents used were acquired from Sigma-Aldrich.

Samples were cultured for 2, 7, and 15 days. The culture medium was changed every 3 days. Culture viability in terms of growth, migration, and cell morphology were evaluated daily. At the end of the procedure, the samples were used to prepare the histological sections.

2.4. Histological section preparation

Samples were fixed in a solution of 4% paraformaldehyde (Synth, SP, Brazil) in 0.01 M phosphate buffer, pH 7.4, for 24 h, after which they were routinely processed for inclusion in Histosec (Merck, Darmstadt, Germany). Longitudinal sections (7 µm thick) were prepared as previously suggested [23–25].

2.5. Research groups and outline

This study included five groups of six samples each. The control groups, consisting of uncultured dHAM and limbus fragments, were called NC-HAM and NC-L, respectively. The experimental groups, consisting of dHAM and limbus constructs, were called C-2, C-7, and C-15, with the numbers referencing the number of days in culture.

Optical anisotropy phenomena were studied in four sections from each sample in which six microscopy fields (images) were evaluated. In total, 864 analyses were performed (432 birefringence and 432 LD analyses). Superficial and deep stromal areas were examined in the limbus of all groups. The dHAM evaluations were performed on the ECM of the stromal areas underlying the basal membrane. The evaluation fields were randomly chosen for NC-HAM. In the C-2, C-7, and C-15 groups, the analysis was restricted to regions supporting the limbal explant and/or the epithelial cells that migrated from it, as seen in Fig. 1.

Biomedical Optics EXPRESS

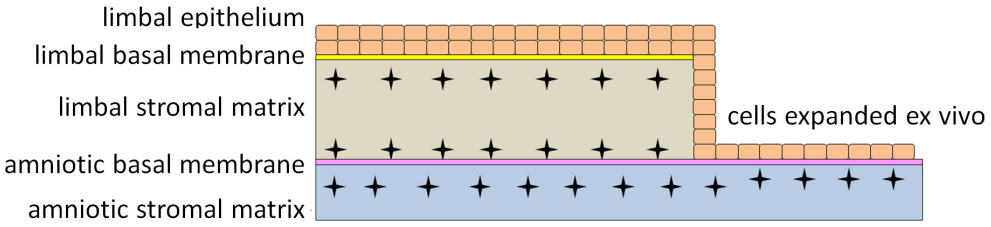

Fig. 1. Schematic representation of the amniotic and limbal stromal areas examined in the C-2, C-7, and C-15 groups regarding the optical anisotropy parameters that inform on the supramolecular organization of fibrillar collagen and proteoglycans. ✦, examined areas.

2.6. Birefringence parameters

Histological sections were stained with Ponceau SS acidic solution (Sigma-Aldrich), pH 2.5, for 3 min as previously suggested [37]. The evaluations were conducted on an Olympus BX-53P polarized light microscope (Olympus, Tokyo, Japan) equipped with 10 × and 40 × UPLFLN objectives, a 546-nm monochromatic band-pass filter, and a halogen lamp. Working conditions, namely light intensity, were identical for all samples. With the help of a video camera, the images were transmitted from the microscope to a computer, where they were digitalized.

The digitalized images were converted to a binary system (8-bit colors) containing 256 grey levels (GA) varying from zero to 255, and analyzed using Image J software (http://imagej.nih.gov/ij/; National Institutes of Health, Bethesda, MD, USA). The procedures described by Vidal and Mello [24] was used to calibration of the image analysis system. The intensity of the birefringence brightness was studied in fibers positioned at about 45 degrees from the PPL [23–25]. The image segmentation process was performed manually. The images were divided in quadrants for the in situ quantification of the average values of GA (in pixels), the maximum GA values (GAmax), and the minimum GA values (GAmin). The birefringence brightness contrasts were expressed using the following formula: average GAmax values – average GAmin values [26].

Interference colors caused by anomalous birefringence dispersion were studied in collagen fibers visualized under polychromatic conditions, that is, the monochromatic filter was removed from the light path. Interference colors were associated with the thickness of the fibers. Yellow and red shines were attributed to thicker fibers, while green was attributed to thin fibers (20–40 nm) [38].The percentage of birefringent areas covered by fibers shining in different colors was calculated using Image J software.

2.7. Dichroic parameters

Histological sections were stained with 0.025% toluidine blue solution (Sigma-Aldrich) in 0.1M Mcllvaine buffer, pH 4.0, for 15 min, as previously described [23, 33].The evaluations were conducted on an Olympus BX-53P polarized light microscope (Olympus) equipped with a 40 × UPLFLN objective, a halogen lamp, Köhler illumination and monochromatic light of different wavelengths, and a video camera. Working conditions, namely light intensity, were identical for all samples.

To study spectral absorption and LD, the analyzer filter was removed from the light path and the polarizer was kept in the field. Absorptiometric studies were sequentially performed using 500, 520, 540, 560, 580 and 600 nm wavelength photons. For each wavelength, the longitudinal axis of the histological section was positioned both perpendicular and parallel to the PPL. Absorption measurements (in arbitrary units, AU) were performed using an image analysis software (Image J) in calibrated optical density mode. The slide's background without any biologic material was used to calibrate the system (100% transmittance). Spectral absorption curves were created in which the average perpendicular (APE) and parallel (APA) absorption values to the PPL against the wavelength of the photon were plotted. LD values

Biomedical Optics EXPRESS

were calculated at the maximum absorption points of the curves using the formula APA – APE [23].

2.8. Statistical analysis

The Chi-square test was used to compare the qualitative variables between the different groups. Analysis of variance, Tukey's test and Kruskall-Wallis were used to compare continuous quantitative variables. The results are expressed as mean ± standard error of the mean (SEM), or as median and range. Differences were considered significant at values of $p \leq 0.05$.

3. Results

3.1. Cell culture

The cells started to grow by 2–5 days of culture. In this time, they were smaller and better defined, with a 1:2 nucleus-cytoplasm ratio. As migration occurred (at 7 days of culture), the cell layer demarcation became clear with a 1:3, 1:4 nucleus-cytoplasm ratio. The evolution of the cell expansion area is shown in Fig. 2.

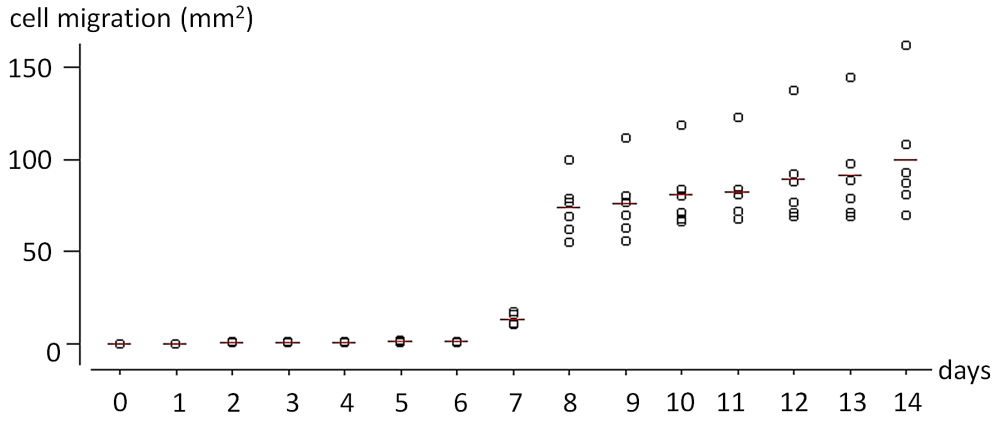

Fig. 2. Dotplot of epithelial cell migration area over time for rabbit limbal explants cultured on denuded amniotic membranes. Means are indicated by lines.

3.2. Birefringence parameters

Table 1 shows the means and SEM established for the GA, GAmax, and GAmin values quantified in the dHAM and limbal collagen fibers.

Regarding the amniotic stromal ECM, the C-2, C-7, and C-15 groups presented with lower GA and GAmin values than those of the NC-HAM group ($p<0.001$). GAmax values of C-7 did not differ from the control ($p>0.05$). As for the limbal stromal ECM, C-7 showed elevated GA values compared to NC-L ($p<0.001$). Conversely, C-15 showed reduced GA values ($p<0.05$). The GAmax values for all of the cultured limbal samples differed from those of the NC-L group (C-2, $p<0.01$; C-7 and C-15, $p<0.01$), while the GAmin values were elevated in the C-2 and C-7 groups ($p<0.001$).

The NC-L collagen fibers showed reduced GA values, in pixels, compared to those of the NC-HAM collagen fibers ($p<0.001$). In samples cultured for 2 and 7 days, GA values of the limbal collagen fibers were higher than those of the amniotic fibers ($p<0.001$ for all).

The birefringence brightness contrasts of the amniotic collagen fibers were 2.0 in NC-HAM, 13.25 in C-2, 19.26 in C-7, and 13.23 in C-15. Regarding limbal collagen fiber brightness, the contrasts were 23.01 in NC-L, 13.39 in C-2, 19.90 in C-7, and 30.31 in C-15.

Biomedical Optics EXPRESS

Table 1. Video image analysis parameters related to the birefringence brightness intensity (expressed as grey level and derivatives, in pixels) of amniotic and limbal collagen fibers from 7-µm sections stained with Ponceau SS and illuminated with monochromatic polarized light (wavelength from 546 nm)

Parameter	Groups			
	Amniotic stromal collagen fibers			
	NC-HAM	C-2	C-7	C-15
GA (pixels)	92.90 ± 0.23	86.48 ± 0.38‡	90.34 ± 0.45‡	87.20 ± 0.59‡
GAmax	93.50 ± 0.30	88.21 ± 0.32‡	93.20 ± 0.61	88.63 ± 0.74‡
GAmin	91.50 ± 0.15	74.96 ± 0.37‡	73.94 ± 0.36‡	75.40 ± 0.13‡
	Limbal stromal collagen fibers			
	NC-L	C-2	C-7	C-15
GA (pixels)	89.35 ± 0.10	88.61 ± 0.90	95.02 ± 0.18‡	85.05 ± 0.39*
GAmax	91.50 ± 0.31	90.34 ± 0.54†	98.80 ± 0.28‡	98.80 ± 0.46†
GAmin	68.49 ± 0.13	76.95 ± 0.10‡	78.90 ± 0.38‡	68.29 ± 0.11

NC-HAM, uncultured de-epithelialized human amniotic membrane fragment; NC-L, uncultured limbal fragment; C-2, 2-day culture group; C-7, 7-day culture group; C-15, 15-day culture group; GA, grey average; GAmax, maximum GA value; GAmin, minimum GA. Data are expressed as mean ± SEM. * $p<0.05$ versus controls; † $p<0.01$ versus t controls; ‡ $p<0.001$ versus controls.

Following illumination with polychromatic polarized light, the amniotic and limbal collagen fibers showed green, yellow, and/or red interference colors [Appendix, Fig. 4]. The proportion of collagen fibers shining in the different colors is presented in Table 2.

Table 2. Proportion (%) of green, yellow, and red collagen fibers detected in the birefringence images stained with Ponceau SS and illuminated with polychromatic polarized light.

Interference colors Anomalous dispersion of birefringence	Groups			
	Amniotic stromal collagen fibers			
	NC-HAM	C-2	C-7 *	C-15 *
Green fibers	75.00	80.66	61.78	51.68
Yellow fibers	22.30	16.31	31.01	21.66
Red fibers	2.70	3.03	7.21	26.66
	Limbal stromal collagen fibers			
	NC-L	C-2 *	C-7 *	C-15
Green fibers	40.54	30.41	41.52	37.95
Yellow fibers	39.55	48.34	51.41	34.42
Red fibers	19.91	21.25	17.07	27.63

NC-HAM, uncultured de-epithelialized human amniotic membrane fragment; NC-L, uncultured limbal fragment; C-2, 2-day culture group; C-7, 7-day culture group; C-15, 15-day culture group
The Chi-square test revealed differences in interference colors of C-7 and C-15 versus NC-HAM as well as of C-2 and C-7 versus NC-L . * $p<0.05$ versus the uncultured controls

Differences were detected between the interference colors of C-7 and C-15 amniotic collagen fibers versus the NC-HAM group ($p<0.05$), and the C-2 and C-7 limbal collagen fibers versus the NC-L ($p<0.05$).

3.3. Dichroic parameters

Figure 3 corresponds to the spectral absorption curves constructed for research sample after toluidine blue staining. The amniotic stromal ECM, in all groups, showed different points of maximum polarized light absorbance (480–500, 540–560, 580–600 nm), which coincided between APE and APA. APE and APA values of the C-2, C-7, and C-15 groups were higher than those of the NC-HAM group for all wavelength photons ($p<0.001$). Regarding limbal ECM, the APE and APA values of the C-15 group were higher than those of the NC-L group for all wavelength photons ($p<0.01$), except 560 nm.

Biomedical Optics EXPRESS

In all of the research groups, absorbance values observed in the ECM of the dHAM (APE range, 0.65–1.4 AU; APA range, 0.5–1.37 AU) were higher than those observed in the limbal ECM (APE range, 0.33–0.82 AU; APA range, 0.32–0.84 AU) ($p<0.001$).

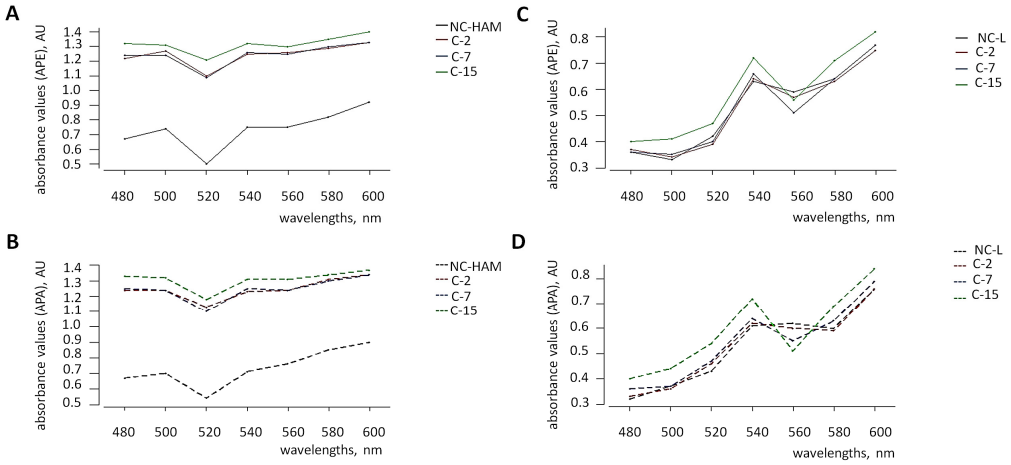

Fig. 3. Spectral absorption curves generated for amniotic (A and B) and limbal (C and D) stromal extracellular matrices after toluidine blue staining. The mean perpendicular absorption (APE) (A and C) and parallel absorption (APA) (B and D) values were plotted against the different photon wavelengths. AU, arbitrary units.

LD values, calculated at the maximum spectral absorbance points of the amniotic and limbal ECM of the studied groups, are listed in Table 3. LD values were negative in the control samples (NC-HAM and NC-L groups) and alternated between positive and negative values in the cultured samples.

Table 3. Linear dichroism (LD) values calculated at the maximum absorbance points observed in the spectral curves created for the research groups.

Wavelength	Groups			
	Amniotic stromal matrix			
	NC-HAM	C-2	C-7	C-15
	LD	LD	LD	LD
480-500 nm	–0.04	–0.03	0.00	0.01
540-560 nm	–0.04	–0.02	0.01	0.01
580-600 nm	–0.02	0.01	0.01	0.03
	Limbal stromal matrix			
	NC-L	C-2	C-7	C-15
	LD	LD	LD	LD
540 nm	–0.02	–0.02	–0.02	0.00
600	–0.01	0.01	0.02	–0.02

NC-HAM, uncultured de-epithelialized human amniotic membrane fragment; NC-L, uncultured limbal fragment; C-2, 2-day culture group; C-7, 7-day culture group; C-15, 15-day culture group. T LD is negative when the average perpendicular absorption value exceeded the average paralel absorption value

4. Discussion

The present study evaluated the supramolecular organizations of the dHAM and limbal ECM before and after explant culture. Phenomena resulting from the interactions of the supra-organized ECM with electromagnetic radiation constituted the physical basis of the performed

Biomedical Optics EXPRESS

analyses. As expected, we observed that the incidence of polarized electromagnetic waves on the amniotic and limbal ECMs led to changes in the phase and amplitude of the orthogonal components of the electric vector, generating anisotropic and spectral optical effects.

The results of this study revealed that the culture procedure–induced stimuli altered the anisotropical and supra-organizational properties of the dHAM and limbal ECM. Changes in supra-organization can be explaned by the fact that the ex vivo ECM undergoes constant synthesis and degradation, as well as modifications in molecular composition [39]. The supra-organizational alterations here observed arising of the combination of multiple individual stimuli, such as composition of culture medium and forces exerted by the cells outgrowing of the limbal explant.

Previous studies [26, 40–42] showed that anisotropy could be considered a measurement of the degree of order of nematic liquid crystals, which are formed of elongated and flexible molecules and display a certain spatial orientation. We have advocated that the limbus and dHAM stroma correspond to physiologically active and highly dynamic liquid-crystalline systems capable of changing the orientation and interaction of its elements according to the morpho-functional requirements received. The liquid crystal concept has been widely used to describe other structures such as the cornea, bones and tendons [26, 40–42]. It is especially based on the observation that fibrillar collagens (baton-shaped) show mesophasogenic characteristics and piezo/pyroelectric properties.

Fibrillar collagens are highly bright second harmonic generator, and can be considered as periodic and ordered nanostructures able to altering the propagation of polarized light by exhibiting nonlinear optical properties [43]. Many polarized light-based techniques are disponible to studying collagen fibers, including polarizing microscopy [44].

Among several advantages of studying collagen with polarized light microscopy is the fact that information on fiber orientation obtained in the X-Y Cartesian bidimensional plane can be added to brightness intensity (birefringence) in the Z-plane [23, 24, 26, 43]. In order to obtain threedimensional information from the collagen birefringence, the simplest approach could be the analysis of variation of brightness intensity as a function of the long axis of the collagen fibers relative to the PPL, in a similar way to that proposed to solve problems of Fourier filtering [24, 26, 43]. The information contained in the X-Y-Z coordinate plane are related to molecular order, concentration, spatial direction, and ordered aggregational states of anisotropic biopolymers [43].

Usually, no staining is required when studying collagen fibers with polarized light microscope. However, in this study, the collagen fibers formed a complex with Ponceau SS, an azo dye that aligns its resonating electrons in parallel with the collagen, amplifying the birefringence signal [23, 37]. The macromolecular complexes formed by the interaction of Ponceau SS with collagen have characteristics of photonic material [45], and can provide a basis for understanding the relationships between mesophase organization and functionality in biological structures [37, 45].

Birefringence brightness intensity was evaluated by quantifying GA and its derivatives (GAmax and GAmin). GA is a densitometric parameter that is correlated with the optical difference path (OPD) measured by phase compensators [26]. It is known that the higher the OPD or GA values of a birefringent sample, the greater the number of electronic variations (crystallinity) and/or cross-links [23]. The number of cross-links determines the alignment, stability, and ordered states of aggregation of the collagen fibers and is positively correlated with the stiffness of the tissue [22–26, 46, 47].

In this study, NC-L collagen fibers showed lower GA values than did NC-HAM collagen fibers. This finding shows that the limbal and amniotic fibrillar collagens differ with regard to crystallinity and/or packing degree.

A key concept in ECM biology regards how the supra-organizational and biomechanical properties of the ECM can influence cellular activities [48]. It is noteworthy that, before the start of cell migration, the GA values of the amniotic collagen fibers in samples cultured for 2 and 7 days were lower than those obtained for the limbal collagen fibers. In C-15 group, however, it was observed an increase of the mean GA of the amniotic collagen fibers. It is

Biomedical Optics EXPRESS

possible that this finding represents a morpho-functional requirement that stimulus LEPCs to migrate from limbus to dHAM. We are currently studying this hypothesis by evaluating the formation/positioning of focal adhesion and the expression of integrins in LEPCs in vivo and ex vivo.

Amniotic collagen fibers of C-2, C-7, and C-15 groups presented with lower GA values (suggestive of lower stiffness) than those of the NC-HAM group. Indeed, supra-organization and stiffness of ECM are crucial properties by the which cells senses external forces and respond to the microenvironment cues [49]. All these properties are interconnected and one can influence the other. It is not therefore not surprising that alterations in amniotic ECM supra-organization can have a important impact on the cell functionallity. In favor, a recent work showed enhanced functions from differentiated stem cells on softer susbtrates [50]. In previous studies, Tseng [51] demonstrated that mammary gland epithelial cells migrate from regions of higher tension to those of lower tension in an attempt to reduce the anisotropic stress in its surroundings.

The contrast in birefringence brightness represents an important collagen supra-organization parameter and reflects alterations in fiber-related undulation and spatial orientation [26]. In this study, NC-HAM collagen fibers showed homogeneous brightness (2.0 contrast), whereas NC-L fibers showed heterogeneous brightness (23.01 contrast). These results indicate that the dHAM (cryopreserved as in this research) contain collagen fibers that preferentially oriented in a single spatial direction, that is, along its structural axis. Limbal collagen fibers, as expected, showed more than one preferential direction, forming different angles within the stroma in addition to a lamellar structure [52–54].

Interestingly, culturing the cells caused changes in the direction and spatial plane of the dHAM collagen fibers. The brightness contrast values of the amniotic fibers increased to levels close to those obtained for limbal fibers, especially in the C-2 and C-7 groups. Since it is assumed that limbal explant culture mantains the various cells present in the limbal stroma close to the basal epithelial cells [55, 56], we believe that mechanical forces derived from the stromal cells modulated the spatial orientation of collagen remodeling.

Interference colors caused by anomalous birefringence dispersion, a non-linear optical phenomenon, were associated with collagen fiber thickness [38, 57].

Associations between interference colors and collagen types were not established (even though type III collagen, present in amniotic ECM in high quantities, is thinner than type I collagen, present in the limbal ECM) because type I collagen fibers, when immature or obliquely cut, are bright green [38, 57, 58].

Changes in the proportion of thin/green and thick/red fibers were observed after cell culture procedures. Previous studies showed that this finding may indicate altered collagen fiber maturation degree [57]. We believe that the presence of thick/red fibers in the amniotic ECM of cultured samples is a reflection of changes in turnover (and probably in procollagen conversion and lysyl oxidase enzyme activity), which is in accordance with the supra-organization states revealed by the GA measurements.

Collagen fiber thickness and diameter are associated with the generation and transmission of forces that facilitate cell junction repositioning [59–61]. PGs, via their GAGs, constitute mechanisms that control fiber diameter. Additionally, they form a bridge between adjacent collagen fibers, facilitating their sliding when a force is applied [60]. Studies on optical phenomena, such as selective light absorption and LD, have been conducted in an attempt to further our knowledge of the interaction between PGs and collagen [23, 31–33, 35].

Similar to other biological macromolecules, PGs show no LD in the visible light spectrum. Therefore, toluidine blue dye was used in the present study to extrinsically promote LD [33]. Toluidine blue binding to PG GAGs is characterized by metachromatic reactions that are represented by the absorbance peaks observed in spectral curves [31–33].

Amniotic membrane ECMs (all groups) showed three absorbance peaks (520, 540, and 580–600 nm) and limbal ECMs showed two polarized light absorbance peaks (540 and 600 nm). Detection of the different peaks suggested that GAGs of PG with varying levels of aggregation were bioavailable to bind to toluidine blue, which supports the findings of

Biomedical Optics EXPRESS

previous studies involving other structures that sustain the simultaneous action of compression and tension forces [23, 32, 62].

It was previously demonstrated that GAGs of PGs are aligned in parallel with the longitudinal axis of the fibrillar collagen, and this alignment generates a negative LD in samples stained with toluidine blue [23, 33, 35, 63]. Negative LD values were detected for stromal ECM of NC-HAM and NC-L, confirming the results already reported for other anisotropic structures [23, 33, 35]. After cell culture, however, alterations were detected in the dichroic signal of the studied ECMs, suggesting spatial GAG reorientation. The LD values in the C-2, C-7, and C-15 groups alternated between positive and negative values. This observation allows us to propose that the ordered interaction between GAGs and fibrillar collagens is a statistical event that depends on extrinsic spatial and temporal requirements. The causes of the spatial GAG reorientation as observed in this research remain unknown, but the bonds that are established between these molecules and those of toluidine blue are considered electrostatic. It is possible that the electric field generated by the fetal calf serum, a component of the culture medium, acted on the intermolecular electronic transitions.

As a limitation, in this study, we did not determine the contributions of each tissue culture stimulus to the supramolecular (anisotropical) alterations observed. We also do not determine the impact of the supra-organizational alterations for the functionality of the ECM and the cultured LEPCs (this was not an objective of the research). Our results encourage future studies to investigate possible pathways cell-ECM interaction triggered by supramolecular requirements.

5. Conclusions

We have demonstrated that the supra-organizations of fibrillar collagens and PGs of dHAM and limbal stromal PGs are labile and suffer alterations during tissue culture procedures. Our findings are relevant for cell therapies and tissue bioengineering since the component rearrangements of the supra-organized ECM may constitute microenvironmental regulation mechanisms by which cells are modulated.

Biomedical Optics EXPRESS

6. Appendix

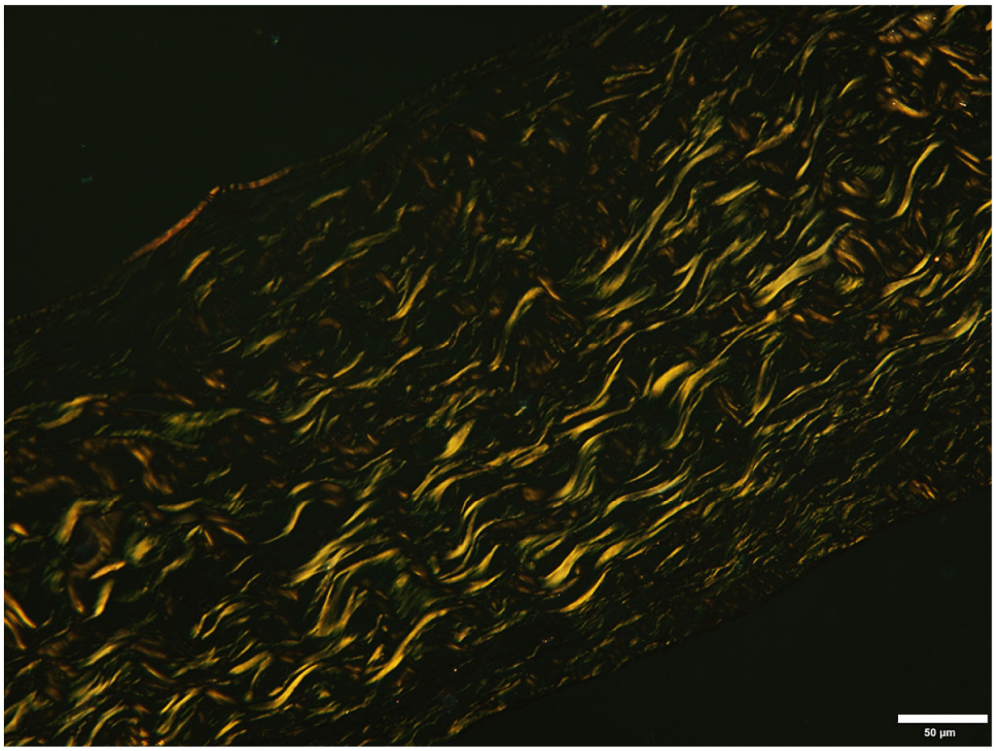

Fig. 4. Photographic image of interfence colors observed in one of the research samples.

Funding

Funding was provided by the São Paulo Research Foundation – FAPESP (Proc. 2012/17308-5, Proc. 2013/01494-7, Proc. 2013/25533-1), and the National Council for Scientific and Technological Development – CNPq (Proc. 467289/2014-0).

Acknowledgments

Gisele P. Valdetaro and Marcela Aldrovani contributed equally to this work. We would like to Tiago Barbalho Lima and Roberta Martins Crivelaro for their help with anesthesia and postoperative care of the rabbits. This manuscript is a part of the Master's thesis of Gisele P. Valdetaro.